

# Lawrence Berkeley National Laboratory

## Energy Storage & Distributed Resources

### Title

Metalation and coordination reactions of 2 H-meso-trans -di( p -cyanophenyl)porphyrin on Ag(111) with coadsorbed cobalt atoms

### Permalink

<https://escholarship.org/uc/item/2gs6w30r>

### Journal

Physical Chemistry Chemical Physics, 20(38)

### ISSN

0956-5000

### Authors

Kuliga, Jan  
Zhang, Liang  
Lepper, Michael  
[et al.](#)

### Publication Date

2018-10-03

### DOI

10.1039/c8cp05255g

Peer reviewed



Cite this: *Phys. Chem. Chem. Phys.*,  
2018, 20, 25062

# Metalation and coordination reactions of 2*H*-*meso*-*trans*-di(*p*-cyanophenyl)porphyrin on Ag(111) with coadsorbed cobalt atoms†

Jan Kuliga,<sup>ab</sup> Liang Zhang,<sup>ab</sup> Michael Lepper,<sup>ab</sup> Dominik Lungerich,<sup>bc</sup>  
Helen Hölzel,<sup>bc</sup> Norbert Jux,<sup>bc</sup> Hans-Peter Steirück<sup>ab</sup> and  
Hubertus Marbach<sup>id</sup>\*<sup>ab</sup>

We investigated the metalation and coordination reactions of Co with 2*H*-5,15-bis(*para*-cyanophenyl)-10,20-bisphenylporphyrin (2*Htrans*DCNPP) on a Ag(111) surface by scanning tunneling microscopy. At room temperature (RT), 2*Htrans*DCNPPs self-assemble into a supramolecular structure stabilized by intermolecular hydrogen bonding. The metalation of 2*Htrans*DCNPP is achieved either by depositing Co atoms onto the supramolecular structure at RT, or, alternatively, by depositing the molecules onto a submonolayer Co-precovered Ag(111) surface with a subsequent heating to 500 K. In addition, the molecules coordinate to Co atoms through the N atoms in the peripheral cyano groups with a preference of isolated 4-fold coordination motifs at RT.

Received 17th August 2018,  
Accepted 14th September 2018

DOI: 10.1039/c8cp05255g

rsc.li/pccp

## Introduction

The investigation of functional molecules on solid surfaces has become a vivid research field in fundamental and applied sciences, with the goal to fabricate novel molecular based devices. The rational design of functional molecular architectures *via* surface-confined coordination chemistry was identified as a promising route to target this goal.<sup>1,2</sup> Such systems represent a new class of functional materials, which promise unique functionalities from unsaturated metal centers and/or the molecular ligands. A particularly promising family of molecular building blocks are porphyrins with functional peripheral substituents.<sup>3–10</sup> Related studies mainly focused on relevant surface reactions such as the direct metalation of the porphyrin macrocycle, coordination of additional ligands and cross-linking *via* surface coordinative bonds.<sup>3–8</sup>

The reaction of porphyrins with coadsorbed metal atoms under ultrahigh vacuum (UHV) conditions is especially interesting for the *in situ* synthesis of reactive metalloporphyrins

such as iron(II)-tetraphenylporphyrins. The latter are difficult to handle outside the vacuum, due to their high affinity toward oxygen.<sup>11,12</sup> The metalation is a redox reaction and has been studied for a variety of porphyrins, with different substituents and with different metals, such as Ce,<sup>13</sup> Co,<sup>6,7,14</sup> Cu,<sup>15–20</sup> Fe,<sup>11,12,21</sup> Ni<sup>22,23</sup> and Zn.<sup>14,24</sup> In a combined experimental and theoretical study of this complex reaction, it was initially proposed that the metal atom is first coordinated to the four N atoms of the intact porphyrin, and thereafter, the two aminic hydrogen atoms are successively transferred to the metal center, where they recombine and desorb as molecular hydrogen (H<sub>2</sub>).<sup>14</sup> However, for 2*H*-tetraphenylporphyrins (2HTPP) on a Cu(111) surface, it was recently demonstrated by means of temperature-programmed desorption that the hydrogen atoms are not directly released as H<sub>2</sub> into the gas phase, but are first transferred to the substrate and associatively desorb from there.<sup>19</sup> The theoretical studies of this reaction mechanism in a gas phase reaction predict that Fe and Co species react with porphyrin at RT, whereas elevated temperatures are required for Cu and Zn atoms, as confirmed in various experimental studies on adsorbed porphyrins.<sup>6,7,11,12,14,21,24</sup> Besides metalation of porphyrins coadsorbed metal atoms can also be utilized to interlink porphyrins *via* metal–organic bond formation on the surface.<sup>5,8,25–28</sup>

In this work, we report on the self-assembly and reaction of 2*H*-5,15-bis(*para*-cyanophenyl)-10,20-bisphenylporphyrin (2*Htrans*DCNPP) with coadsorbed Co atoms on a Ag(111) surface investigated by scanning tunneling microscopy (STM). We show that deposition of Co atoms on the surface pre-covered with

<sup>a</sup> Lehrstuhl für Physikalische Chemie II, Friedrich-Alexander-Universität Erlangen-Nürnberg, Egerlandstr. 3, 91058 Erlangen, Germany.  
E-mail: hubertus.marbach@fau.de

<sup>b</sup> Interdisciplinary Center for Molecular Materials (ICMM), Friedrich-Alexander-Universität Erlangen-Nürnberg, Nikolaus-Fiebiger-Str. 10, 91058 Erlangen, Germany

<sup>c</sup> Lehrstuhl für Organische Chemie II, Friedrich-Alexander-Universität Erlangen-Nürnberg, Nikolaus-Fiebiger-Str. 10, 91058 Erlangen, Germany

† Electronic supplementary information (ESI) available: Detailed evaluation of molecular arrangement of 2*Htrans*DCNPP on Ag(111). See DOI: 10.1039/c8cp05255g

*2HtransDCNPP* results in metalation of the molecules at RT. In addition, the metalated porphyrins also coordinate with Co atoms through the N atoms of the cyano groups at RT; annealing at 400 K enhances the process. However, no supramolecular metal–organic coordination network formation is observed.

## Experimental

The experiments and sample preparations were performed in a two-chamber ultrahigh vacuum (UHV) system with a base pressure of  $\sim 10^{-10}$  mbar. The microscope is an RHK UHV VT STM 300 with RHK SPM 100 electronics. The STM images were acquired at RT in constant current mode with a Pt/Ir tip. The given bias voltages refer to the sample. The STM images were processed with WSxM software and moderate filtering (Gaussian smooth, background subtraction) was applied for noise reduction. The Ag(111) single crystal was prepared by repeated cycles of Ar<sup>+</sup> sputtering (500 eV) and annealing to 850 K. The *2HtransDCNPP* molecules were deposited onto the Ag substrate at RT by thermal sublimation from a home-built Knudsen cell at 690 K. The coverage of the *2HtransDCNPP* monolayers on the Ag substrate was determined by STM. The molecular models were optimized with the MM2 force field calculation method implemented in Chem & Bio 3D.

## Results and discussion

The deposition of *2HtransDCNPP* on Ag(111) at RT gives rise to the close-packed and well-ordered supramolecular structure shown in Fig. 1, which reflects a subtle balance between intermolecular and molecule–substrate interactions.<sup>5,11,29</sup> The lattice vectors of the unit cell are  $a = 1.61 \pm 0.04$  nm and  $b = 2.65 \pm 0.03$  nm, with an enclosed angle  $\gamma = 90 \pm 3^\circ$ ; see Fig. 1b. This unit cell yields a molecular density of 0.47 molecules per nm<sup>2</sup> which corresponds to a coverage of 0.034 ML, with a ML defined as one adsorbate molecule or atom per substrate surface atom. Notably, about  $\sim 85\%$  of the surface is covered with this structure, with the rest of the surface uncovered which results in an effective coverage of  $\sim 0.029$  ML.

In order to further elucidate the arrangement of *2HtransDCNPP*s, the appearance of individual molecules in STM images has to be clarified first. Fig. 1c shows a close-up STM image of one molecule incorporated in a two-dimensional island; the same image is also shown in Fig. 1d with a scaled overlay of a space filling model of *2HtransDCNPP*. Similar to the intramolecular conformation of *2HTPP*<sup>11,29</sup> and *2H-5,10,15,20-tetrakis(para-cyanophenyl)porphyrin* (*2HTCNPP*)<sup>25</sup> on Ag(111), *2HtransDCNPP* appears as four protrusions in the periphery around a core with a depression in the center. The four protrusions show different lateral size, with two opposite protrusions larger and the other two smaller. From the molecular dimensions we assign the former to the cyano-phenyl groups and the latter to the “bare” phenyl groups. The good agreement between the STM image and the scaled molecular model in Fig. 1d further corroborates this assignment along with a detailed analysis documented in the ESI.†

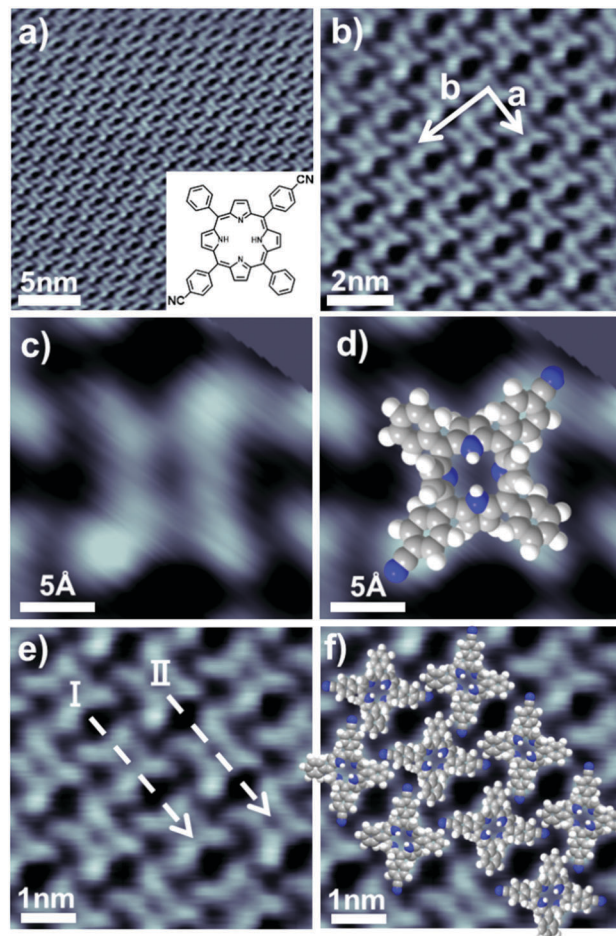


**Fig. 1** (a and b) Constant current STM images of the self-assembled *2HtransDCNPP* on Ag(111). A unit cell is also overlaid in (b). (c) Close up STM image of one *2HtransDCNPP* molecule, and (d) the same image overlaid with the corresponding scaled space filling model. (e) Magnified detail of the center part of (a), and (f) the same image overlaid with the correspondingly scaled molecular models. Tunneling parameters:  $U = -0.1$  V,  $I = 27$  pA.

With the interpretation of the appearance of individual *2HtransDCNPP* molecules, the supramolecular arrangement within the islands is analyzed in detail. Fig. 1e shows a high resolution STM image clearly resolving the sub-molecular features in the structure. To facilitate the identification of both supramolecular and intramolecular features, the image is superimposed with scaled models of *2HtransDCNPP* (Fig. 1f): all molecules within a row (I) are oriented along the same direction while this azimuthal orientation switches by  $90^\circ$  in the neighboring rows (II). (The orientation of individual molecules is determined by the position of cyano groups.) Consequently, in every second row the molecules have the same molecular orientation. This supramolecular structure is likely to be stabilized by van der Waals interactions and intermolecular hydrogen bonding between terminal nitrogen atoms in the cyano group and hydrogen atoms of pyrrole groups of adjacent molecules in the neighboring rows.<sup>15,30</sup> It should be noted that for *2HTPP* on Ag(111), the molecules self-assemble in domains with a square

unit cell caused by the T-type intermolecular interactions between the peripheral phenyl substituents of neighboring molecules.<sup>29</sup> This is obviously not the case for *2Htrans*DCNPP studied here. Closer inspection reveals, that the cyano groups “avoid” direct neighborhood, which can be understood by simple electrostatic considerations. In this regard the attachment of the cyano groups is obviously suitable to significantly influence the intermolecular interactions and thus to tailor the resulting supramolecular structure to some extent.

As next step, we deposited  $0.012 \pm 0.003$  ML of Co, which is stoichiometrically roughly one third of the amount required to metalate all porphyrins on the surface (1 ML is defined as one adsorbate per substrate surface atom). Following Co deposition, a fraction of the molecules appear as protrusions in the STM images, while the others remain unchanged, see Fig. 2a. The observed protrusions are in line with an enhanced tunneling contribution through the Co(II)  $3d_{z^2}$  orbitals and are a strong indication for metalation of the *2Htrans*DCNPP molecules with Co to CotransDCNPP.<sup>3,31</sup> The fraction of CotransDCNPP (31%) is in good agreement with the amount of deposited Co.

The STM images of Fig. 2b and c were acquired after the successive deposition of equal amounts of  $0.012 \pm 0.003$  ML Co onto the molecules, yielding 0.024 and 0.036 ML of deposited Co, respectively. The number of protrusions, that is CotransDCNPP molecules, increases roughly proportional to the amount of codeposited Co: the fraction of metalated molecules in Fig. 2 are (a) 31%, (b) 73% and (c) 97%; these numbers have to be compared to the values expected for a stoichiometric reaction which are (a) 41%, (b) 82% and (c) 120%, considering the effective starting coverage of 0.029 ML for *2Htrans*DCNPP. Comparing these values under consideration of the margin of error (25% of the amount of deposited Co) it becomes immediately clear that the efficiency of the metalation reaction is close to 100%.

Notably, the supramolecular structure is maintained during the described metalation, despite the known affinity of CN groups to Co atoms favoring the formation of metal-organic networks at RT with related linkers.<sup>27,28,32</sup> As the evaporation of

Co atoms on the surface is a statistical process, it can be ruled out that all Co atoms directly adsorb at the center of a *2Htrans*DCNPP molecule. Therefore, at least some of the Co atoms have to diffuse to the corresponding sites and then metalate the molecules.<sup>3</sup> Similar observations were also reported for Co/2HTPP/Ag(111),<sup>6,7</sup> Fe/2HTPP/Ag(111),<sup>11,12</sup> Fe/2H-tetrapyrrolylporphyrin/Ag(111),<sup>33</sup> Fe/2H-octaethylporphyrin (2HOEP)/Ag(111),<sup>34</sup> Ni/2HOEP/Cu(111),<sup>35</sup> Co/2H-tetra(4-cyanophenyl)phenylporphyrin (2HTPCN)/Ag(111)<sup>27</sup> and Co/2HTPCN/BN/Cu(111).<sup>28</sup>

Further increase of the amount of deposited Co to 0.072 ML, which is stoichiometrically more than double the amount of Co needed for full metalation of the porphyrin layer, leads to a breakup of the supramolecular structure into a variety of disordered intermolecular arrangements, as is shown in Fig. 3a. This process is even more pronounced after annealing at 400 K, after which most molecules have formed disordered clusters or cannot be imaged any more (Fig. 3b). Since the disordered clusters emerge exclusively upon the codeposition of excessive Co, we conclude that they must involve Co atoms. Previous studies of codeposited Co atoms and cyano-functionalized polyphenyl molecules demonstrated the formation of ordered metal-organic networks where each Co atom coordinates to three molecules with an angle of  $120^\circ$  between each other.<sup>26,32</sup> Notably, upon depositing more molecules than required for a saturated honeycomb mesh, 4-, 5- and 6-fold coordination of Co atoms was observed, which goes along with various pore shapes.<sup>32</sup> More relevant are the findings by Urgel *et al.*, who reported that cyano-functionalized porphyrins form 3-fold prevailed metal-organic coordination motifs with codeposited Co atoms on a Ag(111).<sup>27</sup> Based on the overall similarity of the latter system and *2Htrans*DCNPP, we propose that the disordered clusters found after the deposition of over-stoichiometric Co amounts is due to the formation of Co-CotransDCNPP coordination compounds. Apparently, the stepwise deposition of Co first leads to metalation of the free-base *2Htrans*DCNPP at RT with high efficiency. Upon increasing the total amount of Co on the surface significantly above the stoichiometrically amount needed to metalate all molecules we propose the formation of Co-coordinated

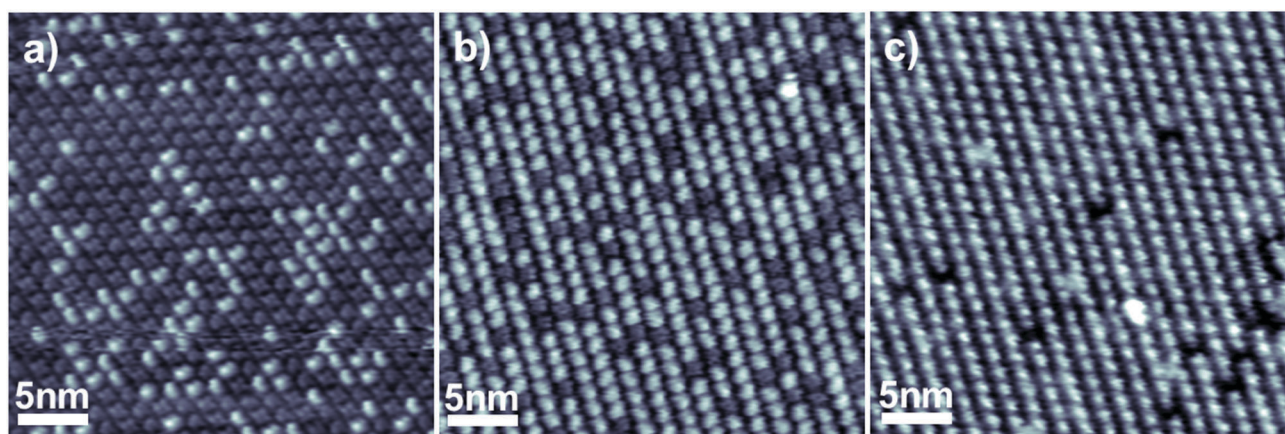


Fig. 2 Constant current STM images of a monolayer of *2Htrans*DCNPP molecules after the incremental deposition of Co (0.012 ML in each step). Tunneling parameters:  $U = -1.0$  V,  $I = 29$  pA.

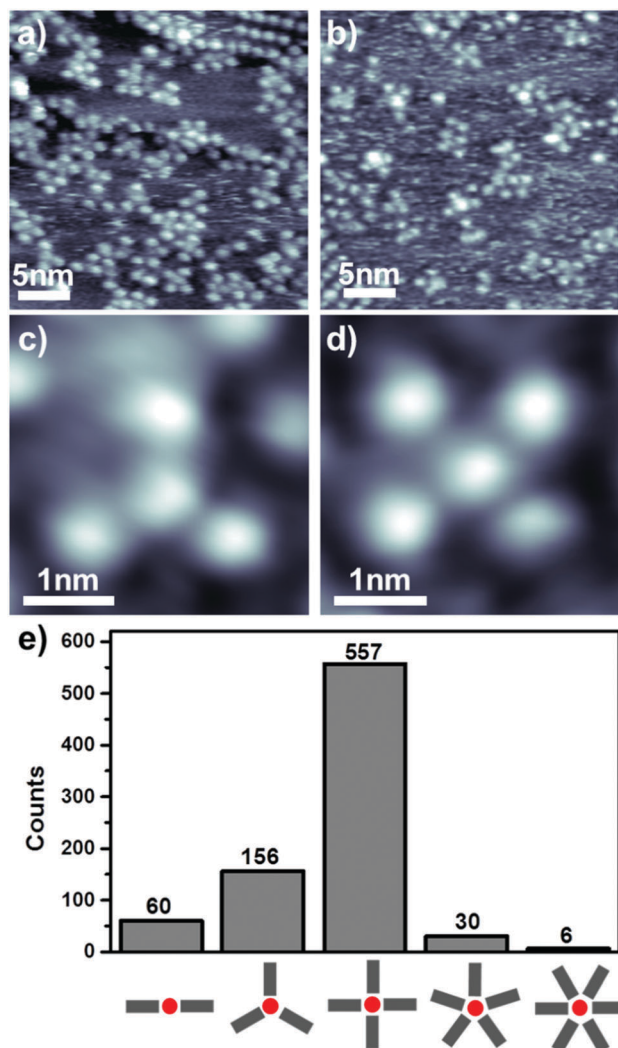


Fig. 3 (a) STM image of amorphous metal–organic structure of metalated 2*H*transDCNPP (CotransDCNPP) and Co formed at RT. (b) STM image of the amorphous coordination structure observed after annealing the sample to 400 K. (c and d) STM images of two representative coordination motifs observed in experimental results; (e) distribution of the number of CotransDCNPP molecules coordinating to a Co atom. Tunneling parameters:  $U = -1.0$  V,  $I = 29$  pA.

CotransDCNPP structures. However, these coordination structures lead to a breaking up of the ordered supramolecular arrangement. While the preceding metalation occurs at RT and without further thermal treatment, the proposed subsequent coordination is promoted by 400 K annealing. One simple way to understand this behavior is that for the metalation the Co atoms can easily diffuse to the porphyrins bound in the supramolecular structure at RT. However, additional thermal energy for the rearrangement of molecules is needed, *e.g.*, to overcome activation barriers for diffusion, to realize the formation of the observed coordination structures.

Fig. 3c and d display the STM images of two representative motifs observed in our study. All observed motifs (see Fig. 3e) have in common that two to six protrusions are arranged around one central protrusion (marked in red in Fig. 3e). The average

distance of an “outer” protrusion to a central protrusion is  $1.0 \pm 0.1$  nm irrespective of the actual motif.

This estimated distance is much too small to identify all protrusions with CotransDCNPP molecules. This is evident, considering the lattice parameter  $a = 1.61 \pm 0.04$  nm estimated for the molecular order discussed in detail above. As discussed above, at the given negative bias voltages, *i.e.*, sensitive to the HOMO of the CotransDCNPP molecules, the appearance of a central round protrusion is fully expected. This can be explained by a strong contribution of an orbital-mediated tunneling process *via* the hybrid  $\text{Co}(d_{z^2})\text{-Ag}$  orbital of the adsorption complex, induced by molecule–substrate interactions.<sup>3,31</sup> We speculate that a Co atom coordinated by two to six nitrogen atoms from cyano groups might exhibit a similar appearance as a Co atom coordinated by four nitrogen atoms in the porphyrin macrocycle. Based on the latter consideration in combination with the short protrusion–protrusion distances we propose that the central protrusions are Co atoms coordinated by the cyano groups of surrounding CotransDCNPP molecules. This interpretation is also supported by a control experiment without deposition of Co, in which only the closed packed arrays of molecules were observed after the corresponding annealing procedure. To verify our interpretation STM images at the same position with both negative and positive bias voltages were acquired. The motivation of this course of action is that at positive bias voltage the corresponding STM images of Co-porphyrins rather reflect the topography of the molecules than the pronounced electronic effect at negative bias. It should be mentioned that the corresponding experiments are extremely demanding, nevertheless we could acquire some conclusive data as depicted in Fig. 4.

In the upper two rows of Fig. 4 two examples of bias switching (first column: negative bias, second column: positive bias) along with the corresponding STM images overlaid with scaled models (third column). Fig. 4a depicts one of the most frequently observed five-protrusion motifs acquired at negative bias voltage. The exact same region of interest is depicted in Fig. 4b, now at positive bias voltage. From this STM image one can clearly identify the four outer protrusions in Fig. 4a as CotransDCNPP molecules, while no porphyrin is observed in Fig. 4b at the position of the central protrusion in Fig. 4a. Instead a rather small protrusion is observed which we assign to Co. The corresponding arrangement is depicted in Fig. 4c with the superimposed scaled molecular models and the Co center indicated as red dot. Again, it should be mentioned that the acquisition of such polarity switching STM images is extremely demanding and time consuming in our instrument. This is probably due to unintended tip modifications due to the bias switching in combination with the existence of mobile material at room temperature. In this regard it should be pointed out, that the observed motif deviates from the vast majority of other five-protrusion motifs, since the characteristic distances in the particular case shown in Fig. 4a–c is with  $1.2 \pm 0.1$  nm somewhat enlarged in comparison to the average value of  $1 \pm 0.1$  nm. The typical distance is resembled by the STM images shown in Fig. 4d–f. However, in that case the central spot is missing at negative bias as depicted in Fig. 4a.

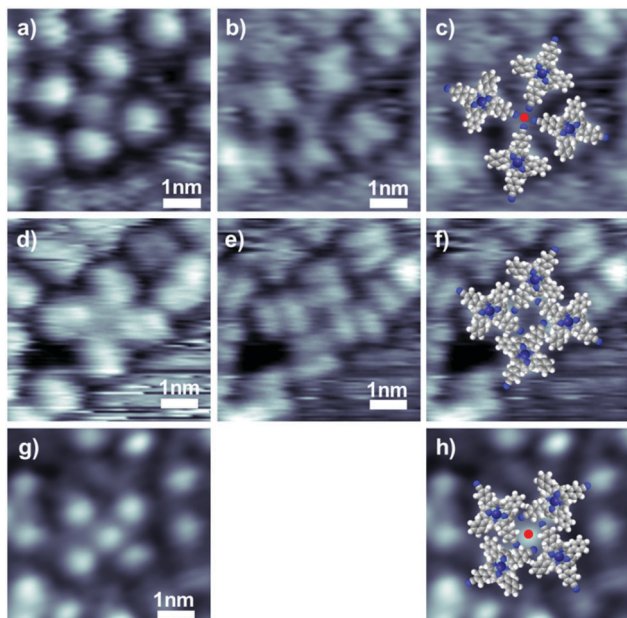


Fig. 4 Bias dependent STM measurements. The first column (a, d and g) presents images measured with negative bias. The second column (b and e) depicts the images measured at the same position but with positive bias. In the third column (c, f and h) the images are presented with overlaid scaled models. Tunneling parameters: (a and d)  $U = -1.0$  V,  $I = 29$  pA. (b and c)  $U = +1.0$  V,  $I = 29$  pA. (e)  $U = +1.7$  V,  $I = 29$  pA. (g and h)  $U = -0.1$  V,  $I = 30$  pA.

This is again referred to a specific tip modification, since all motifs at this measurement appeared without the central protrusion at negative bias, which reappeared on the same preparation after some time and a presumed tip change. However, in the latter case it was not possible to image at positive bias. Fig. 4g reproduces Fig. 3d in which the four outer protrusions have the same arrangement and measurements. We therefore conclude that the underlying molecular arrangement is also identical. The corresponding conformation is revealed by the STM image acquired at positive bias depicted in Fig. 4e. Here an “windmill” arrangement is observed (see Fig. 4f and h). We propose that this arrangement is indeed the dominating motif since it also resembles a distance of the center of the CotransDCNPP molecules to the center of the supramolecular arrangement, *i.e.* the position of the central Co atom of  $1 \pm 0.1$  nm. It should be mentioned that the oxidation state of Co in CotransDCNPP and in coordination nodes might be different.<sup>15,28</sup> Indeed, in analogy to free Co-TPP,<sup>6</sup> an oxidation state of 2+ is assumed for isolated CotransDCNPP, while the Co coordination nodes might maintain the 0 oxidation state of isolated adatoms,<sup>28</sup> which might explain that the central coordinating Co atom is invisible in Fig. 4d. Based on the presented evidence along with a lack of plausible alternative explanations we conclude that the observed features are indeed CotransDCNPP molecules linked *via* Co atoms.

It is interesting to note that these metal–organic coordination motifs do not form extended 2D networks with the metalated CotransDCNPP in our experiments. We speculate that the absence of long-range order as observed here might be related

to the symmetry and lattice mismatch between the coordination structure and the hexagonal substrate.<sup>27</sup> Another possibility might be that we did not explore the right preparation parameters, *i.e.*, that the observed coordination motifs are kinetically trapped.<sup>36</sup>

For further insight into the formed organic-metal coordination compounds, a statistical analysis of  $\sim 800$  molecules was performed. The distribution of coordination numbers is shown in Fig. 3e. Motifs ranging from 3-fold up to 6-fold coordination can be found, with the 4-fold coordination dominating the scheme. Additional Co clusters found on the terraces exclude the shortage of metal atoms as a possible reason for the diverse coordination structures.<sup>32</sup> We propose that the 4-fold coordination bond is stronger than the other coordination bonds, but the energy difference between them is not sufficient to significantly favor one binding motif (4-fold) over the others (2-, 3-, 5-, 6-fold).<sup>36</sup> Note that metal dimer, trimers, and possibly larger clusters could constitute the coordination nodes, and therefore the coordination number depends on the cluster size.<sup>36–38</sup> However, there is no experimental evidence to support this hypothesis and so far the literature reports unanimously agree that cyano groups coordinate to only one metal center.<sup>26–28,32</sup> Notably, the appearance of 5- and 6-fold lateral coordination is surprising considering steric limitations, and could indicate that the CotransDCNPP molecules in these coordination motifs are not flat-lying but are tilted with respect to the surface due to the repulsion between neighboring molecules or even that involved molecules are actually damaged, *e.g.*, are missing a side group or the likes.

Based on the discussion above, we conclude that the 2*Htrans*DCNPPs are metalated and coordinated by post-deposited Co atoms at the porphyrin core and the peripheral cyano groups, respectively. A next logical step is to explore these reactions by changing the sequence of the deposited materials, that is, to first deposit the metal and then the porphyrins. Fig. 5a and b show the STM images of a Ag(111) surface before and after the deposition of  $\sim 0.1$  ML of Co at RT. The result reveals that Co atoms form three-dimensional islands which decorate the atomic steps on the Ag(111) surface.

After the deposition of roughly a closed monolayer 2*Htrans*DCNPP onto the Co precovered Ag(111) at RT, a homogeneous adlayer of 2*Htrans*DCNPP is observed on terraces, in addition to the Co cluster at the steps, (Fig. 5c). The molecules show the same supramolecular structure as on clean Ag(111). The coexistence of Co clusters and the porphyrin molecules in the undisturbed island structure indicates that the metalation reaction at RT is very slow at the given conditions.

Interestingly, heating to 500 K leads to the partial formation of CotransDCNPP, as shown Fig. 5d. The bright species are assigned to CotransDCNPP (43%) and the dim species to 2*Htrans*DCNPP (57%). The required annealing step indicated that in the clusters the Co atoms are relatively strongly bound and consequently heating is necessary to dissolve the Co clusters and make the individual Co atoms available for metalation *via* diffusion to a 2*Htrans*DCNPP molecule. In other words, metalation with pre-deposited Co atoms is kinetically hindered,

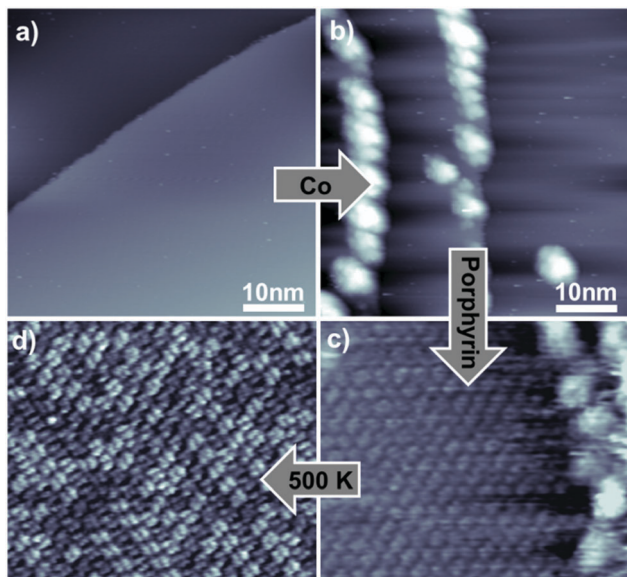


Fig. 5 (a) STM image of the clean Ag(111). (b) STM image showing the nucleation of Co on step edges of Ag(111). (c) *2HtransDCNPP* monolayer prepared via vapor deposition onto the surface depicted in Fig. 4b. (d) Situation after heating the surface shown in Fig. 4c to 500 K. The bright spots in the image are assigned to CotransDCNPP formed by metalation of *2HtransDCNPP*. Tunneling parameters: (a)  $U = -1.0$  V,  $I = 29$  pA; (b)  $U = -1.3$  V,  $I = 30$  pA; (c and d)  $U = 1.0$  V,  $I = 30$  pA.

and heating is necessary to overcome the kinetic hindrance.<sup>3,11,24</sup> At higher heating temperatures, the supramolecular ordering is totally degraded, and the uniform shape of the molecules is no longer present (not shown). This is most likely due to the decomposition of the molecules. As a consequence, no metal–organic coordination structures are observed.

## Conclusions

We have demonstrated that *2HtransDCNPP* molecules on Ag(111) exhibit a bifunctional behavior toward coadsorbed Co atoms. In a first step, the molecules react with Co atoms through the four N atoms in the macrocycle under formation of CotransDCNPP. If Co is deposited onto *2HtransDCNPP*s, the reaction proceeds rapidly and efficiently at RT; if Co is deposited first, the metalation reaction requires elevated temperatures. As a second step, the peripheral cyano groups can also coordinate with Co atoms with a preferred 4-fold coordination motif, but also 3-fold, five-fold and six-fold motifs. The metal–organic coordination structures appear at RT and annealing at 400 K enhances the coordination process.

## Conflicts of interest

There are no conflicts to declare.

## Acknowledgements

The authors gratefully acknowledge the funding by the German Research Council (DFG) through research unit FOR 1878/funCOS,

the Cluster of Excellence ‘Engineering of Advanced Materials’ (<http://www.eam.uni-erlangen.de>) and by the Collaborative Research Center SFB 953 at the Friedrich-Alexander-Universität Erlangen-Nürnberg. L. Z. thanks the Alexander von Humboldt Foundation for a research fellowship. M. L. and D. L. thank the Graduate School Molecular Science (GSMS) for financial support.

## Notes and references

- J. V. Barth, G. Costantini and K. Kern, *Nature*, 2005, **437**, 671–679.
- L. Bartels, *Nat. Chem.*, 2010, **2**, 87–95.
- H. Marbach, *Acc. Chem. Res.*, 2015, **48**, 2649–2658.
- H. Marbach and H.-P. Steinrück, *Chem. Commun.*, 2014, **50**, 9034.
- J. M. Gottfried, *Surf. Sci. Rep.*, 2015, **70**, 259–379.
- J. M. Gottfried, K. Flechtner, A. Kretschmann, T. Lukaszczuk and H.-P. Steinrück, *J. Am. Chem. Soc.*, 2006, **128**, 5644–5645.
- J. M. Gottfried and H. Marbach, *Z. Phys. Chem.*, 2009, **223**, 53–74.
- W. Auwärter, D. Écija, F. Klappenberger and J. V. Barth, *Nat. Chem.*, 2015, **7**, 105–120.
- L. Zhang, M. Lepper, M. Stark, D. Lungerich, N. Jux, W. Hieringer, H.-P. Steinrück and H. Marbach, *Phys. Chem. Chem. Phys.*, 2015, **17**, 13066–13073.
- M. Lepper, L. Zhang, M. Stark, S. Ditze, D. Lungerich, N. Jux, W. Hieringer, H.-P. Steinrück and H. Marbach, *J. Phys. Chem. C*, 2015, **119**, 19897–19905.
- F. Buchner, K. Flechtner, Y. Bai, E. Zillner, I. Kellner, H.-P. Steinrück, H. Marbach and J. M. Gottfried, *J. Phys. Chem. C*, 2008, **112**, 15458–15465.
- F. Buchner, V. Schwald, K. Comanici, H.-P. Steinrück and H. Marbach, *ChemPhysChem*, 2007, **8**, 241–243.
- A. Weber-Bargioni, J. Reichert, A. Seitsonen, W. Auwärter, A. Schiffrin and J. Barth, *J. Phys. Chem. C*, 2008, **112**, 3453–3455.
- T. E. Shubina, H. Marbach, K. Flechtner, A. Kretschmann, N. Jux, F. Buchner, H.-P. Steinrück, T. Clark and J. M. Gottfried, *J. Am. Chem. Soc.*, 2007, **129**, 9476–9483.
- Y. Li, J. Xiao, T. E. Shubina, M. Chen, Z. L. Shi, M. Schmid, H.-P. Steinrück, J. M. Gottfried and N. Lin, *J. Am. Chem. Soc.*, 2012, **134**, 6401–6408.
- M. Stark, S. Ditze, M. Lepper, L. Zhang, H. Schlott, F. Buchner, M. Röckert, M. Chen, O. Lytken and H.-P. Steinrück, *Chem. Commun.*, 2014, **50**, 10225–10228.
- L. Zhang, M. Lepper, M. Stark, R. Schuster, D. Lungerich, N. Jux, H.-P. Steinrück and H. Marbach, *Chem. – Eur. J.*, 2016, **3347**–3354.
- K. Diller, F. Klappenberger, M. Marschall, K. Hermann, A. Nefedov, C. Wöll and J. V. Barth, *J. Chem. Phys.*, 2012, **136**, 014705.
- M. Röckert, M. Franke, Q. Tariq, D. Lungerich, N. Jux, M. Stark, A. Kaftan, S. Ditze, H. Marbach, M. Laurin, J. Libuda, H.-P. Steinrück and O. Lytken, *J. Phys. Chem. C*, 2014, **118**, 26729–26736.
- S. Ditze, M. Stark, M. Drost, F. Buchner, H.-P. Steinrück and H. Marbach, *Angew. Chem., Int. Ed.*, 2012, **51**, 10898–10901.

- 21 D. Ecija, M. Trelka, C. Urban, P. D. Mendoza, E. Mateo-Martí, C. Rogero, J. A. Martín-Gago, A. M. Echavarren, R. Otero and J. M. Gallego, *J. Phys. Chem. C*, 2008, **112**, 8988–8994.
- 22 M. Chen, X. F. Feng, L. Zhang, H. X. Ju, Q. Xu, J. F. Zhu, J. M. Gottfried, K. Ibrahim, H. J. Qian and J. O. Wang, *J. Phys. Chem. C*, 2010, **114**, 9908–9916.
- 23 C. Wang, Q. Fan, S. Hu, H. Ju, X. Feng, Y. Han, H. Pan, J. Zhu and J. M. Gottfried, *Chem. Commun.*, 2014, **50**, 8291–8294.
- 24 A. Kretschmann, M. M. Walz, K. Flechtner, H.-P. Steinrück and J. M. Gottfried, *Chem. Commun.*, 2007, 568–570.
- 25 M. Lepper, T. Schmitt, M. Gurrath, M. Raschmann, L. Zhang, M. Stark, H. Hölzel, N. Jux, B. Meyer, M. A. Schneider, H.-P. Steinrück and H. Marbach, *J. Phys. Chem. C*, 2017, **121**, 26361–26371.
- 26 U. Schlickum, R. Decker, F. Klappenberger, G. Zoppellaro, S. Klyatskaya, M. Ruben, I. Silanes, A. Arnau, K. Kern and H. Brune, *Nano Lett.*, 2007, **7**, 3813–3817.
- 27 J. I. Urgel, D. Ecija, W. Auwärter, D. Stassen, D. Bonifazi and J. V. Barth, *Angew. Chem., Int. Ed.*, 2015, **54**, 6163–6167.
- 28 J. I. Urgel, M. Schwarz, M. Garnica, D. Stassen, D. Bonifazi, D. Ecija, J. V. Barth and W. Auwärter, *J. Am. Chem. Soc.*, 2015, **137**, 2420–2423.
- 29 F. Buchner, I. Kellner, W. Hieringer, A. Görling, H.-P. Steinrück and H. Marbach, *Phys. Chem. Chem. Phys.*, 2010, **12**, 13082–13090.
- 30 W. Auwärter, A. Weber-Bargioni, A. Riemann, A. Schiffrin, O. Gröning, R. Fasel and J. V. Barth, *J. Chem. Phys.*, 2006, **124**, 194708.
- 31 F. Buchner, K. G. Warnick, T. Wölfle, A. Görling, H.-P. Steinrück, W. Hieringer and H. Marbach, *J. Phys. Chem. C*, 2009, **113**, 16450–16457.
- 32 U. Schlickum, F. Klappenberger, R. Decker, G. Zoppellaro, S. Klyatskaya, M. Ruben, K. Kern, H. Brune and J. Barth, *J. Phys. Chem. C*, 2010, **114**, 15602–15606.
- 33 W. Auwärter, A. Weber-Bargioni, S. Brink, A. Riemann, A. Schiffrin, M. Ruben and J. V. Barth, *ChemPhysChem*, 2007, **8**, 250–254.
- 34 Y. Bai, F. Buchner, M. T. Wendahl, I. Kellner, A. Bayer, H.-P. Steinrück, H. Marbach and J. M. Gottfried, *J. Phys. Chem. C*, 2008, **112**, 6087–6092.
- 35 S. Ditze, M. Röckert, F. Buchner, E. Zillner, M. Stark, H.-P. Steinrück and H. Marbach, *Nanotechnology*, 2013, **24**, 115305.
- 36 S. Krotzky, C. Morchutt, V. S. Vyas, B. V. Lotsch, R. Gutzler and K. Kern, *J. Phys. Chem. C*, 2016, **120**, 4403–4409.
- 37 S. Stepanow, M. Lingenfelder, A. Dmitriev, H. Spillmann, E. Delvigne, N. Lin, X. Deng, C. Cai, J. V. Barth and K. Kern, *Nat. Mater.*, 2004, **3**, 229–233.
- 38 F. Bebensee, K. Svane, C. Bombis, F. Masini, S. Klyatskaya, F. Besenbacher, M. Ruben, B. Hammer and T. R. Linderoth, *Angew. Chem., Int. Ed.*, 2014, **53**, 12955–12959.